Effect of testing conditions on the compressive plasticity of bulk metallic glasses

Yunpeng Jiang[a)]
State Key Laboratory of Mechanics and Control of Mechanical, Nanjing University of Aeronautics and Astronautics, Nanjing 210016, China

(Received 19 April 2016; accepted 26 July 2016)

In this paper, the compressive behaviors of Zr-based bulk metallic glass (BMG) were experimentally studied under different testing conditions. To deeply reveal the inherent deformation mechanisms, numerical study was systematically conducted to analyze the shear banding evolution in BMGs, and the effect of testing machine stiffness, contact friction, and sample parallelism on the compressive ductility was therefore elucidated. Among them the effect of contact friction was carefully studied experimentally and the inherent deformation mechanisms was numerically analyzed in terms of the formation of shear bands. Free-volume theory was incorporated into ABAQUS finite element method code as a user material subroutine UMAT. The numerical method was firstly compared with the corresponding experimental results, and then parameter analyses were performed to discuss the impacts of testing conditions on the malleability of the BMG samples. The present work will shed some light on the interpretation of failure mechanisms in BMGs under different loading conditions.

I. INTRODUCTION

Bulk metallic glasses (BMGs) exhibit many superb properties, e.g., exceptionally high strength, large elastic limit, high hardness, good corrosion resistance, and reduced sliding friction, etc., which render them to be regarded as prospective candidates of engineering materials. However, their structural applications are severely stymied by the intrinsic limited plasticity, which is confined to narrow regions that are called shear bands at room temperature below their glass transition temperature. Therefore, the plastic deformation capability should be one of the most important properties for BMGs, and an accurate testing procedure is bound to be of great significance. Since many factors can affect the measured result, understanding their effect on the mechanical performance should be a necessary prerequisite.

In the past decade, many works have been conducted to analyze the reliance of the plasticity of BMGs on the structure factors such as the sample aspect ratio (the ratio of height to width of sample), notch shape, notch configuration, and so on. Due to their convenience and accuracy, the uniaxial compression experiments are commonly adopted to measure the fundamental properties for BMGs. Park et al.[1] determined the stress–strain curves of Zr-based BMG at high strain rates by the compression test at a temperature in the super-cooled liquid region, and carried out finite element method (FEM) calculations for clarifying the role of the solid metal lubricant during compression. Wu et al.[2] experimentally confirmed that with decreasing sample dimension, the compressive plastic strain of a Zr-based BMG increases from near zero to as high as 80% without failure. A concept of critical shear offset is proposed to explain the strong size effect on the enhanced plasticity by taking the shear fracture energy density into account. Wu et al.[3] investigated the quasi-static compressive deformation behavior of a Vitreloy-1 BMG with an aspect ratio of 0.25, and found that the friction and the confinement at the specimen–loading platen interface would result in a dramatic increase in the compressive load, leading to a higher compressive strength. The formation of many strongly interacted, deflected, wavy, or branched shear bands is attributed to the triaxial stress state in the glassy specimens with a smaller aspect ratio. Zhang[4] pointed that the lateral stress induced by friction between the end of the samples and the crosshead of the testing machine plays a minor role in influencing the yield strength, plastic deformability and shear fracture of BMG samples with a large aspect ratio. But the friction effect would become more and more significant with decreasing aspect ratio of BMG samples. Li et al.[5] involved the friction force in their simulations of the mechanical performance of BMG composite rods due to the presence of microsized and nanosized Ta-rich particles. According to the comparison between modeling and experiment result, the friction force value could be reasonably determined. Wu et al.[6] experimentally

Contributing Editor: Jörg F. Löffler
[a)]Address all correspondence to this author.
e-mail: ypjiang@nuaa.edu.cn
DOI: 10.1557/jmr.2016.291

measured the influence of nonparallelism on the compression plasticity of BMG samples, and Wu et al.[7] concluded that the stiffness of testing machine also affects the plastic deformation of brittle BMG specimens. The effects of testing machine stiffness, contact friction, and sample parallelism on the compressive ductility have been discussed qualitatively before, but the inherent mechanisms are still not clearly revealed yet.

In this paper, FEM modeling and compression experiment were performed to analyze the effect of friction force between the samples and testing machine on the plasticity deformation of BMG samples. Free-volume theory will be incorporated into ABAQUS code as a user material subroutine UMAT. The correctness of the numerical procedure is firstly checked by comparing with the measured results, and then the interrelations between the failure mechanism and various parameters are revealed.

II. EXPERIMENTAL PROCEDURE

Zr-based metallic glass ingot with nominal chemical compositions of $Zr_{52.5}Cu_{17.9}Ni_{14.6}Al_{10}Ti_5$ was prepared by arc melting with high purity elements of 99.9 at.% in an argon atmosphere. As-cast samples were produced by suction casting into a cylindrical rod-shape Cu mold with diameters of 3.9 and 80 mm in length. The cylindrical samples with 1.5:1 aspect ratio for compression tests were prepared. Both ends of each specimen were carefully polished to guarantee parallelism and perpendicularity prior to uniaxial compressive testing.

Conventional compression tests were performed to measure the mechanical properties of the Zr-based metallic glass specimens under the INSTRON 2367 testing machine at room temperature in air. To reduce the friction effect, the graphite powder was uniformly coated onto the top and bottom surfaces of the specimens, and the contact surfaces of the testing machine. All the tests were conducted under a constant strain rate of $10^{-4}\ s^{-1}$, and were repeated at least four times. After the tests, all the specimens were examined using scanning electron microscopy (SEM) for their deformation and fracture features.

III. CONSTITUTIVE RELATIONS OF BMGs

The shear band formation and evolution form fundamental deformation mechanism of BMG. At the microscopic level, shear band formation is believed to be associated with evolution of the local structural order. One atomistic mechanism capturing shear band formation and evolution in BMG is the free-volume model proposed by Spaepen[8] and further developed by Steif.[9] From continuum mechanics point of view, the shear band is a result of strain softening and regarded as a strain-localization phenomenon. The free-volume model treats the free volume as the state variable, which controls the structural change at the atomic level in BMG.

The free-volume is a measure of the departure from the ideally ordered structure and regarded as the difference between the average atomic volume in real materials and that in the ideally ordered structure. This model assumes that the macroscopic plastic flow in pure shear case occurs as a result of net forward atomic jumps in the direction of the applied stress. The general flow equation is expressed as

$$\frac{\partial \gamma^{\mathrm{p}}}{\partial t} = 2\varsigma \exp\left(-\frac{\alpha \nu^*}{\nu_{\mathrm{f}}}\right) \exp\left(-\frac{\Delta G^{\mathrm{m}}}{k_{\mathrm{B}} T}\right) \sinh\left(\frac{\tau \Omega}{2 k_{\mathrm{B}} T}\right) \quad , \tag{1}$$

where γ^{p} denotes the shear strain and the left term of the above equation means the shear strain rate; ς is frequency of atomic vibration; α is a geometric factor of order 1; ν^* is the hard-sphere volume of an atom; ν_{f} is the average free volume per atom; ΔG^{m} is the activation energy; Ω is the atomic volume; τ is the applied shear stress; k_{B} is the Boltzmann constant, and T is the absolute temperature. The average free volume ν_{f} is treated as the order parameter and control the structural change in metallic glasses.

The structural rearrangement with applied stress is controlled by competition between a stress-induced disordering and diffusion reordering process. Consequently, the net increase of the free volume is given as

$$\frac{\partial \nu_{\mathrm{f}}}{\partial t} = \nu^* \varsigma \exp\left(-\frac{\alpha \nu^*}{\nu_{\mathrm{f}}}\right) \exp\left(-\frac{\Delta G^{\mathrm{m}}}{k_{\mathrm{B}} T}\right) \left\{\frac{2\alpha k_{\mathrm{B}} T}{\nu_{\mathrm{f}} C_{\mathrm{eff}}} \left(\cosh\left(\frac{\tau \Omega}{2 k_{\mathrm{B}} T}\right) - 1\right) - \frac{1}{n_{\mathrm{D}}}\right\} \quad , \tag{2}$$

where n_{D} is the number of atomic jumps needed to annihilate a free volume equal to ν^* and is usually taken to be 3–10, and the effective elastic modulus is $C_{\mathrm{eff}} = E/3(1 - \nu)$. Where E is the Young's modulus and ν is the Poisson's ratio, and this is still a stress-controlled process. At low stress level, the free volume created by the stress can be readily annihilated and the homogeneous deformation is maintained, while at high stress level, a net increase of the free volume arises and hence shear banding occurs. In the amorphous material, the free volume can be created by the applied loading, and maybe diffused by the thermal activation. The competition between the creation and diffusion process mainly dominates the resulting deformation mode. If the created free volume is immediately annihilated by Brownian motion, a homogeneous deformation will be reached, otherwise the sample deforms inhomogenously.

According to a J_2-type (the second deviatoric stress tensor invariant with the same formula as that of the Mises' stress defined as follows), small strain visco-plasticity framework, the free-volume model can be generalized into multiaxial stress states. The strain rates can be decomposed into the elastic and plastic parts

$$\dot{\varepsilon}_{ij} = \dot{\varepsilon}^{e}_{ij} + \dot{\varepsilon}^{p}_{ij} \quad . \tag{3}$$

The above elastic part $\dot{\varepsilon}^{e}_{ij}$ is described by the general Hooke's law,

$$\dot{\varepsilon}^{e}_{ij} = \frac{1+\nu}{E}\left(\dot{\sigma}_{ij} - \frac{\nu}{1+\nu}\dot{\sigma}_{kk}\delta_{ij}\right) \tag{4}$$

with a characteristic time scale $t^* = \varsigma^{-1}\exp(\Delta G^m/k_B T)$, the plastic part $\dot{\varepsilon}^{p}_{ij}$, i.e., the flow equation can be described as

$$\dot{\varepsilon}^{p}_{ij} = \exp\left(-\frac{1}{\nu_f}\right)\sinh\left(\frac{\sigma_e}{\sigma_0}\right)\frac{S_{ij}}{\sigma_e} \quad , \tag{5}$$

where $S_{ij} = \sigma_{ij} - \sigma_{kk}\delta_{ij}/3$ is the deviatoric stress tensor and $\sigma_e = (S_{ij}S_{ij})^{1/2}$ is the von Mises' stress. It should be noted that a dot over a quantity denotes $\dot{(\square)} = \varsigma^{-1}\exp(\Delta G^m/k_B T)\,(\partial\square/\partial t)$, which will be used in the following expression. The free-volume evolution equation under multiaxial stress states is written as

$$\dot{\nu}_f = \frac{1}{\alpha}\exp\left(-\frac{1}{\nu_f}\right) \left\{\frac{3(1-\nu)}{E}\left(\frac{\sigma_0}{\beta\nu_f}\right)\left(\cosh\left(\frac{\sigma_e}{\sigma_0}\right) - 1\right) - \frac{1}{n_D}\right\} \quad , \tag{6}$$

where $\sigma_0 = 2k_B T/\Omega$ is the reference stress; $\nu_f = \bar{\nu}_f/\alpha\nu^*$ is the normalized free volume, and $\beta = \nu^*/\Omega$.

IV. FEM MODELING

The above constitutive equations are implemented into ABAQUS code by using a user-defined material subroutine UMAT, which is obtained from Gao's work.[10] In this framework, the shear band is described by an *internal state variable*, i.e., the free volume ν_f. The plastic flow stress is supposed to be a function of the effective Mises stress and the free volume at a given spatial point. The evolution of the free-volume field depends on the stress state and the present free-volume field. The state-variable field and the stress field will be computed, the formation of the shear band corresponds to a localized increase in the state variable, and the progression of shear banding can be described by free-volume density that is denoted by the state-dependent variable in ABAQUS package.[11]

The shear band evolution will be carefully discussed to reveal the failure mechanisms in BMGs. The initial aspect ratio of the specimen, i.e., the ratio of the initial height (measured along axis-x) to the initial width (measured along axis-y) is 2 to 1. The authors[12] have already studied the effect of aspect ratio on the ductility of BMGs, but the present simulation does not to give a direct comparison of model and experiment in terms of aspect ratio, and only a qualitative comparison between them will be conducted. The initially un-deformed FEM mesh of this sample shown in Fig. 1 comprises 5000 CPE4R continuum plane-strain elements, here quadrilateral, isoparametric elements are used in the discretization, and reduced integration is used. Since the main features

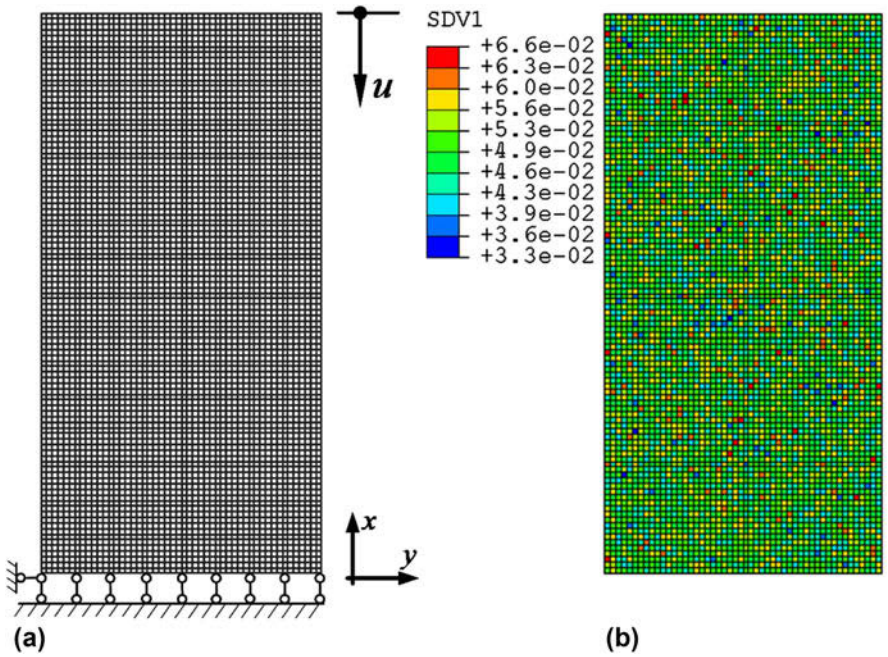

FIG. 1. (a) Finite element mesh consisting of 5000 CPE4R elements for two-dimensional modeling of plane-strain compression and the exerted boundary conditions during the computation, and (b) contour plot of initial value of free volume.

of the shear banding mechanism are better revealed in two-dimensional plane-strain calculations, and thus two-dimensional models are adopted in the whole simulations. During the computation, all the nodes in the bottom node set are prevented from motion along axis-*x*. A negative displacement along axis-*x* is exerted to the single node located at the top-right corner to achieve the desired test strain rate. The multipoint constraint equation is applied to the rest of the nodes in the top surface to keep their deformation coordinate with the top-right corner node. To suppress rigid-body motions of the sample, the node located at the bottom-left corner is prevented from moving along axis-*y*. The remaining nodes in the bottom and top nodes are free to move along axis-*y*.

The prior works[13,14] suggest that the seemly pure BMGs consist of a solid-like region and liquid-like regions in essential, and such the structural heterogeneity in BMGs would result in the nucleation of shear transition zone and the subsequent shear banding progression. Recently, Ding et al.[15] identified soft spots in a BMG, and the atoms in these soft spots participate preferentially in soft vibrational modes and at the same time they have the highest propensity to undergo shear transformations. Jiang[16] also numerically analyzed the dependence of plastic deformation on microstructure inhomogeneity. To better capture the shear localization in the BMG, some elements with a slightly lower value of free volume act as nucleation sites for shear banding. Also shown in Fig. 1(b) is the contour plot for the initial free volume in the BMG sample, and the initial free volume was presumed to be statistically varied over the elements obeying a Gaussian distribution function with a mean value of 0.05, and a standard deviation of 0.005. Unless otherwise noted, all the following numerical simulations for various samples would strictly obey the similar method performed for the specimen as shown here.

It should be emphasized that the main objective of FEM modeling is to better explain the deformation mechanism in the BMGs under various contact conditions. Due to the absence of the exact microstructure characterization, only a qualitative comparison will be conducted between the numerical simulation and experimental results.

V. RESULTS AND DISCUSSION

A. Experimental results and observations

Figures 2 and 3 show the nominal compressive stress–strain curves for the four Zr-based metallic glass specimens without and with using graphite powder, respectively. In the case of no lubrication, the measured results of four samples exhibit good repeatability, and a little plastic deformation happens before the final collapse. The failure strains approximately ranges from 11.8% to 12.5%. Moreover, after yielding, clear serrations in the compression curve are observed, meanwhile many shear bands initiate, nucleate, and propagate, which is contributed to increasing plastic deformation in BMG samples. The shear bands imply a sudden decrease of viscosity, which brings about load drops in the mechanical response. After applying the graphite powder, the main characteristics are similar to those with no lubrication procedure. But what's the most impressive is the remarkable enhancement in the plastic strain deformation. The four samples exhibit a residue plastic strain of nearly 3% as compared to a less than 1% strain for the samples without lubrication.

SEM characterization was used to reveal the difference between the deformation mechanisms under compression with and without lubrication effect.

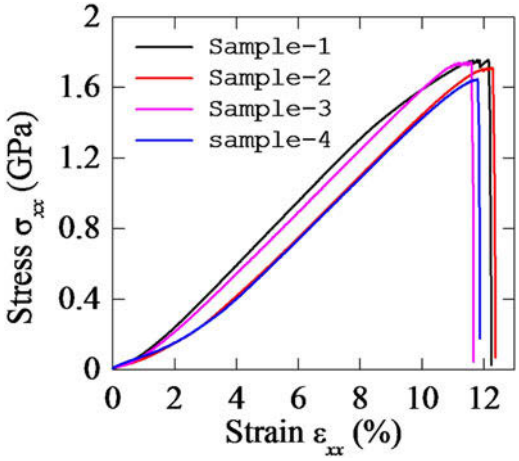

FIG. 2. Nominal compressive stress–strain curves for the four Zr-based metallic glass specimens without using graphite powder.

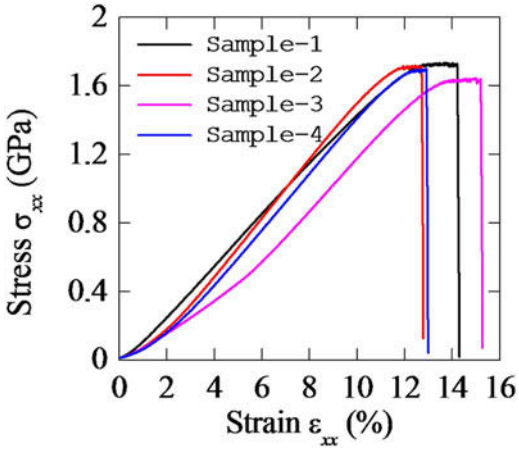

FIG. 3. Nominal compressive stress–strain curves for the four Zr-based metallic glass specimens with using graphite powder.

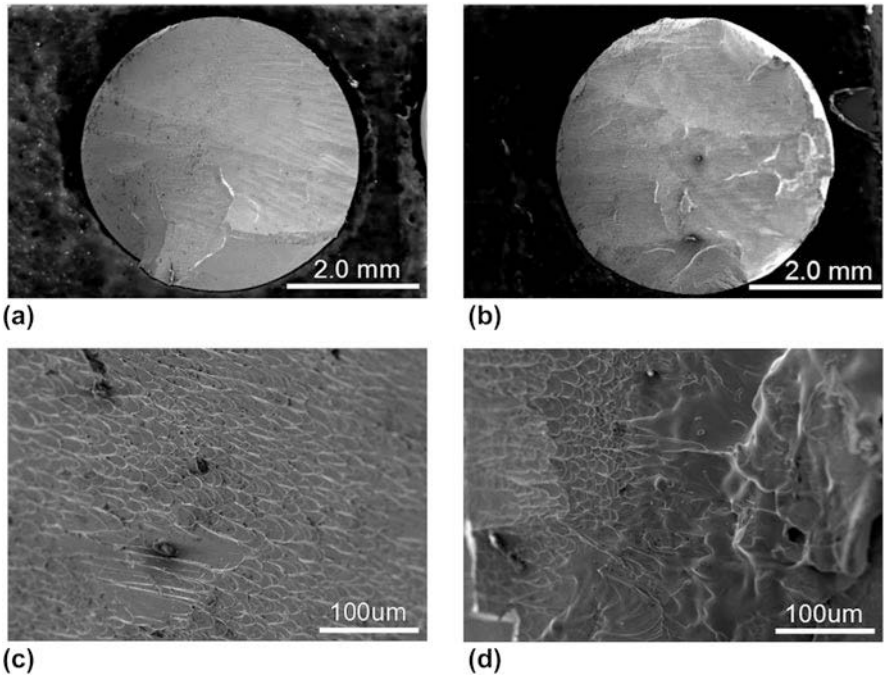

FIG. 4. SEM images on the deformation and fracture morphologies of specimens. (a–c) Specimen without using graphite powder, and (b–d) specimen with applying graphite powder.

The compressive fracture surfaces are shown in Fig. 4 for the samples without and with applying graphite powder, respectively. All the BMGs fractured in a shear mode. The typical feature of the compressive fracture morphology is the vein pattern, and the veins patterns on the compressive fracture surface have an obvious direction. The ductile fracture behavior of the Zr-based BMG exhibits two distinct types of fracture of shear and splitting, which have vein and conchoidal fracture morphologies, respectively. A relatively flat fracture plane with an angle of approximately 42° with respect to the loading axis was covered by vein patterns [Fig. 4(c)], which is the typical BMG shear-fracture feature. After lubricating the BMG samples, the fracture surface becomes relatively rough. Rougher fracture surface is indicative of greater resistance to shear banding propagation. The roughness on the surface implies that a comparatively higher amount of energy was required for the shear band to propagate. Figs. 4(b) and 4(d) show the elongated cellular vein structure at high magnification. This characteristic vein in BMGs indicates that the shear band zone fractured in a relatively ductile mode, but vein patterns shown in Fig. 4(d) seem to indicate a melting state of the material at the shear surfaces, which means that much more heat energy generates for the BMG sample with applying graphite powder.

The profiles for the specimens before and after fracture are shown in Fig. 5. It can be seen that all the BMG samples fractured along the approximate degree 42° against the loading direction. Compared to the sample without applying graphite powders, the side surfaces of BMG specimen become curved after using graphite powders, which means that a larger plastic deformation happened after decreasing the friction force between the machine and BMG samples.

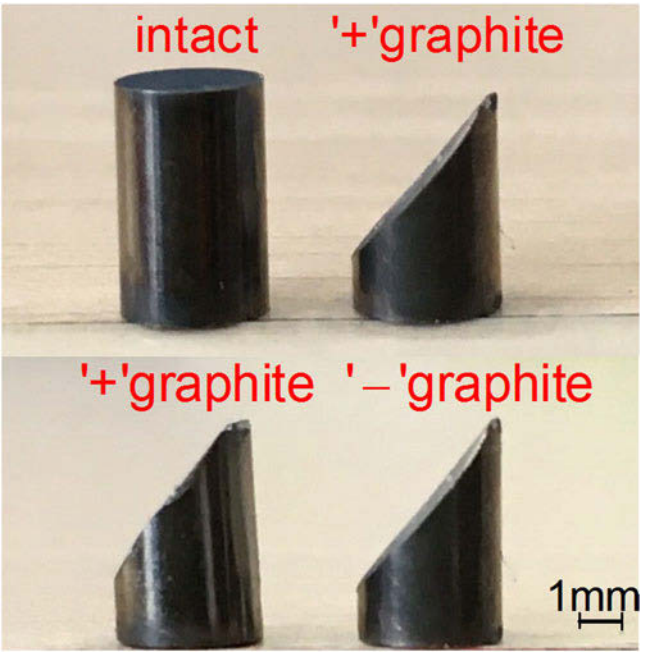

FIG. 5. The profiles of BMG specimens before and after fracture.

B. Verification of the present numerical method

The present FEM modeling is applied to get the stress (σ_{xx})–strain (ε_{xx}) relations in the compression direction for the BMG sample under uniaxial compression. The material properties of BMG will be determined by comparing with the measured stress–strain relations continuously until a satisfied agreement between them is reached. The predictive ability of the FEM method should be firstly checked by comparing with the experimental results.

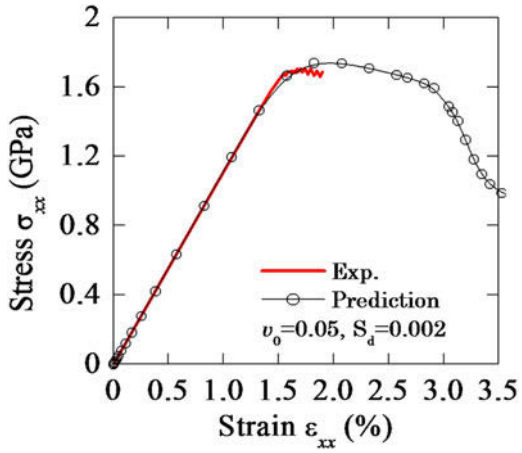

FIG. 6. Comparisons between numerical modeling and the experiments for Zr-based BMG, here 5000 CPE4R elements are meshed.

Fig. 6 shows the comparison between numerical modeling and the experimental results for Zr-based BMG, here element number $N = 5000$ was used. The material properties for the BMG are[17]: $E = 96$ GPa, $\nu = 0.36$, $n_D = 3$, $\alpha = 0.35$, $\beta = 0.85$, and $\nu_f/\alpha\nu^* = 0.085$. Since no damage effect was considered during the simulation, the collapse stage in the deformation response of BMG sample could not be well characterized. However, the main part of the deformation process is in good agreement with the corresponding experimental results, which again confirms the accuracy of the present numerical method. Based on the comparison of modeling and

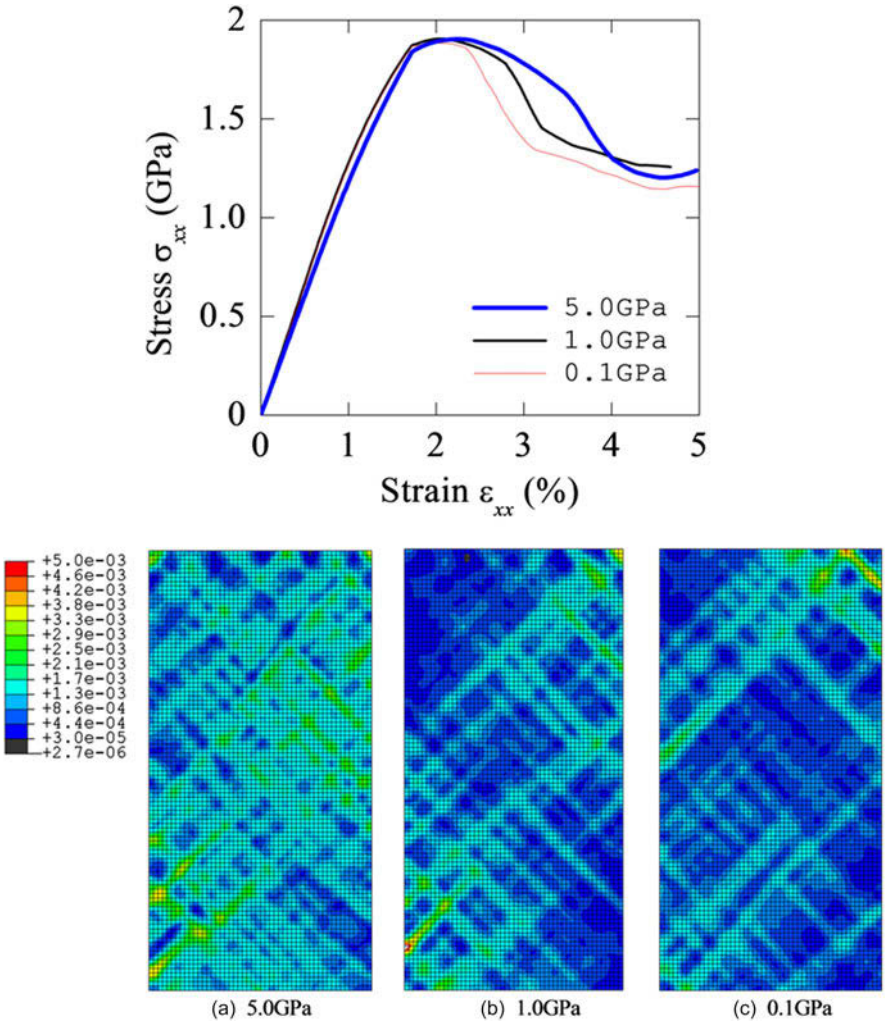

FIG. 7. Effect of testing machine stiffness on the stress–strain relations and the corresponding shear banding evolution in the BMG specimens.

the experimental data, the proposed computational micromechanics model appears to be capable of capturing the main deformation features of BMG materials.

C. Effect of machine stiffness on the compressive plasticity

Figure 7 illustrates the effect of testing machine stiffness on the stress–strain curves and the corresponding shear banding evolution in the BMG specimens. Numerical results show that the uniform plastic deformation improves with enhancing the stiffness of testing machine, and fatherly the corresponding shear banding evolution are given at the applied strain $\varepsilon_{xx} = 3.2\%$. Much more shear bands are induced in the BMG samples under compression with higher testing machine stiffness, and thus more uniform deformation is reached. Wu's experiments[7] also found that, as the machine stiffness increased, the samples exhibited better shear stability, i.e., showing larger compressive plasticity.

D. The effect of friction on the compressive plasticity

Figure 8 shows the reliance of the stress–strain relations on the friction coefficient between the BMG specimens and testing machine, here the top and bottom surfaces are parallel. It is seen from these curves that the uniform deformation of the sample without friction is far larger than those of the others, and reaches up to 7%. While the uniform strains of the other situations are less than 5%. The big difference and the corresponding inherent failure mechanisms could be revealed from the associated contours of shear band propagation as shown in Fig. 9.

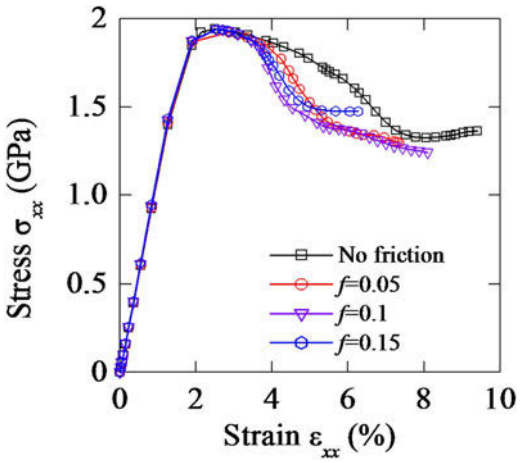

FIG. 8. Dependence of the stress–strain relations on the friction coefficient between the BMG sample and testing machine, here the top and bottom surfaces are parallel.

Figure 9 demonstrates the specific evolution of shear banding in the BMG samples with various friction coefficients between the specimens and testing machine. Only a main shear band appears along the maximum shear stress plane in the BMG samples tested with different friction coefficients, and thus the corresponding plastic deformation is very limited. Conversely, the shear banding evolution in the case of applying graphite powder is quite different. It should be noted that a few shear bands are formed and intersected strongly with each

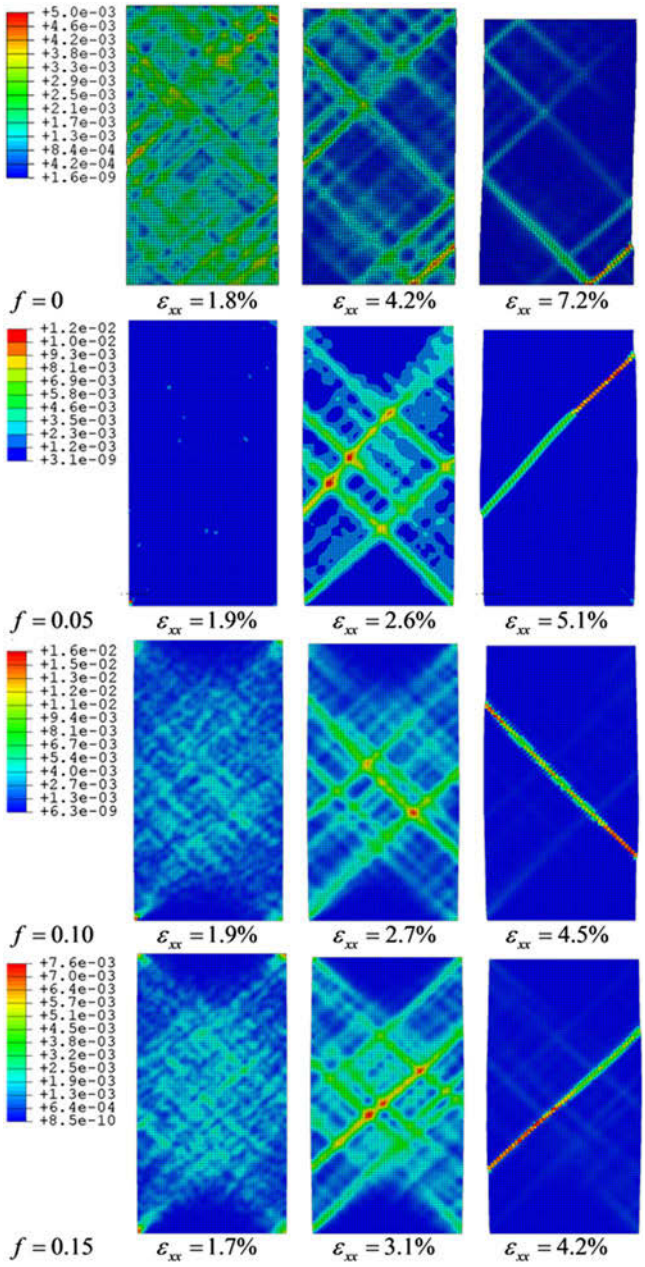

FIG. 9. Contours plot of the shear banding evolution in the BMG samples with various friction coefficients between the specimens and testing machine.

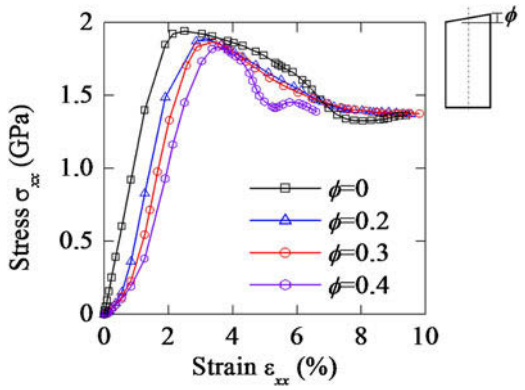

FIG. 10. Dependence of the stress–strain relations on the parallelism between the top and bottom surfaces of BMG sample, here no friction between the sample and testing machine considered.

other, which is called 'blocking effect' in Qu's work.[18] The blocking effect can effectively hinder the rapid propagation of shear banding, and largely delays the stress drop during the deformation process. On the other hand, the large discrepancy among these testing cases could be interpreted as follows. Due to the existence of the friction effect, the up and down surfaces just like two hoops, and strictly restrict the expansion of the local regions. Correspondingly, the local deformation would focus on the middle part of the samples, and thus the probability to induce shear banding and final failure highly increases. Conversely, the application of graphite powder tends to make the sample deform more homogeneously, and more shear bands could be nucleated and propagated.

E. The effect of sample nonparallelism on the compressive plasticity

Figure 10 gives the dependence of the stress–strain relations on the parallelism between the top and bottom surfaces of BMG sample with applying lubrication between the samples and testing machine. The parallelism is defined as the angle ϕ between the top and bottom faces as shown in the associated diagram of Fig. 10. If the up and down surfaces are not parallel, the mechanical response is very different from that of the sample with $\phi = 0$. The fist stage of the stress–strain curve is nonlinear due to the bending deformation of the samples. The present feature is similar to that observation in the experimental results as shown in Fig. 2.

Figure 11 demonstrates the snapshots of the shear banding evolution in the BMG samples with various parallelisms between the top and bottom surfaces of the specimens, and no friction effect is involved. At the very beginning, the samples firstly bend and lean to one side because of the existence of nonparallelism. The shear band also germinates at this side, and gradually propagates to the other side. Finally, one or more shear bands

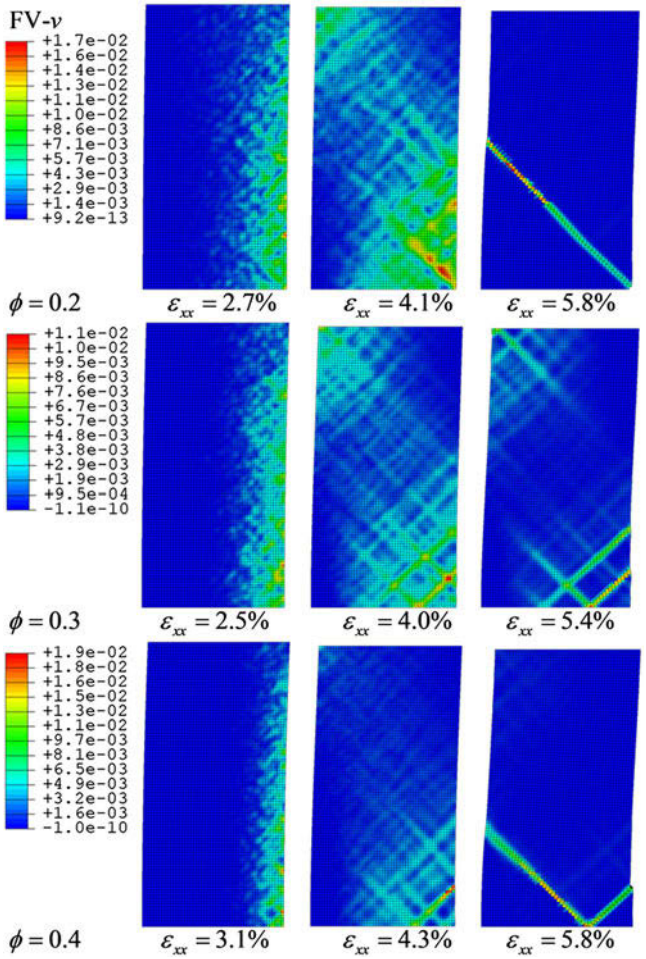

FIG. 11. Contours plot of the shear banding evolution in the BMG samples with various parallelisms between the top and bottom surfaces of the specimens, and no friction effect is considered.

would run through the whole samples, which reach the final collapse. In Wu's experiments,[6] higher plasticity was found to be promoted by geometrical imperfections in the specimen (i.e., miscut or non-orthogonal specimens). These specimens were tilted and bent during testing, leading to a localized geometric confinement which resulted in a false measurement of apparent macroscopic plasticity. These main observations are almost identical to the present simulations as shown in Fig. 11.

VI. CONCLUSIONS

The compression experiment and numerical modeling were used to analyze the shear banding evolution in BMGs under different testing conditions, and correspondingly the relationship between the BMG sample and plasticity behaviors was elucidated. The lubrication effect of applying graphite powder onto the sample surfaces was analyzed in detail. Free-volume theory was incorporated into ABAQUS code as a user material subroutine UMAT. The present numerical method

was firstly compared with the experiments, and then parametric study was performed to reflect the interaction between friction, sample parallelism, and shear bands in the BMG samples. Several main conclusions are reached.

(1) Based on the numerical model with randomly assigned initial free-volume value, the nonparallelism and testing machine stiffness significantly affect the mechanical behaviors of BMG sample.

(2) The friction coefficient between the samples and testing machine largely affect the compressive ductility of BMG samples. After applying the graphite powder, the plastic deformation enhances as compared to that without lubrication.

(3) Based on the free-volume theory, the developed numerical method is capable of elucidating the failure mechanism as observed in the experiments.

(4) The higher stiffness of testing machine is more favorable to improve the compressive plasticity of BMG specimens.

ACKNOWLEDGMENTS

This work was supported by the Fundamental Research Funds for the Central Universities (No. B11020079), Jiangsu Provincial Natural Science Foundation (No. BK2012407), National Natural Science Foundation of China (11202064) and Program for New Century Excellent Talents in University.

REFERENCES

1. E.S. Park, D.H. Kim, H.J. Kim, J.C. Bae, and M.Y. Huh: Plastic stress-strain behavior of a Zr-based bulk metallic glass at high strain rates in the supercooled liquid region. *Mater. Sci. Eng. A* **574**, 54 (2013).
2. F.F. Wu, Z.F. Zhang, S.X. Mao, and J. Eckert: Effect of sample size on ductility of metallic glass. *Philos. Mag. Lett.* **89**, 178 (2009).
3. F.F. Wu, Z.F. Zhang, and S.X. Mao: Compressive properties of bulk metallic glass with small aspect ratio. *J. Mater. Res.* **22**, 501 (2007).
4. Z.F. Zhang, H. Zhang, X.F. Pan, J. Das, and J. Eckert: Effect of aspect ratio on the compressive deformation and fracture behaviour of Zr-based bulk metallic glass. *Philos. Mag. Lett.* **85**, 513 (2005).
5. C. Li, J.S.C. Jang, J.B. Li, D.J. Pan, S.R. Jian, J.C. Huang, and T.G. Nieh: Numerical and experimental studies on the shear band intervention in zirconium based bulk metallic glass composites $Zr_{53}Cu_{22}Ni_9Al_8Ta_8$. *Intermetallics* **30**, 111 (2012).
6. W.F. Wu, Y. Li, and C.A. Schuh: Strength, plasticity and brittleness of bulk metallic glasses under compression: Statistical and geometric effects. *Philos. Mag.* **88**, 71 (2008).
7. F.F. Wu, W. Zheng, S.D. Wu, Z.F. Zhang, and J. Shen: Shear stability of metallic glasses. *Int. J. Plast.* **27**, 560 (2011).
8. F. Spaepen: A microscopic mechanism for steady state inhomogeneous flow in metallic glasses. *Acta Metall.* **25**, 407 (1976).
9. P.S. Steif, F. Spaepen, and J.W. Hutchinson: Strain localization in amorphous metals. *Acta Metall.* **30**, 447 (1982).
10. Y.F. Gao: An implicit finite element method for simulating inhomogeneous deformation and shear bands of amorphous alloys based on the free-volume model. *Modell. Simul. Mater. Sci. Eng.* **14**, 1329 (2006).
11. *ABAQUS Theory Manual* (HKS Inc., Providence, 2010).
12. Y.P. Jiang. *Metall. Mater. Trans. A* **47**, 2481 (2016).
13. H.B. Ke, J.F. Zeng, C.T. Liu, and Y. Yang: Structure heterogeneity in metallic glass: Modeling and experiment. *J. Mater. Sci. Technol.* **30**, 560 (2014).
14. L.S. Huo, J.F. Zeng, W.H. Wang, C.T. Liu, and Y. Yang: The dependence of shear modulus on dynamic relaxation and evolution of local structural heterogeneity in a metallic glass. *Acta Mater.* **61**, 4329 (2013).
15. J. Ding, S. Patinet, M.L. Falk, Y.Q. Cheng, and E. Ma: Soft spots and their structural signature in a metallic glass. *PNAS* **111**, 14052 (2014).
16. Y.P. Jiang: Numerical study of the notch effect on the ductility of bulk metallic glasses (BMGs) based on the free-volume theory. *J. Mater. Res.* **31**, 765 (2016).
17. Y.P. Jiang and K. Qiu: Computational micromechanics analysis of toughening mechanisms of particle-reinforced bulk metallic glass composites. *Mater. Des.* **65**, 410 (2015).
18. R.T. Qu and Z.F. Zhang: Compressive fracture morphology and mechanism of metallic glass. *J. Appl. Phys.* **114**, 193504 (2013).